Lab on a Chip

View Online
Dynamic Article Links

Cite this: *Lab Chip*, 2011, **11**, 1916

www.rsc.org/loc

PAPER

Multiplexed detection of nucleic acids in a combinatorial screening chip†

Benjamin R. Schudel,[ac] Melikhan Tanyeri,[a] Arnab Mukherjee,[a] Charles M. Schroeder*[ab] and Paul J. A. Kenis*[ac]

Received 26th August 2010, Accepted 30th March 2011
DOI: 10.1039/c0lc00342e

Multiplexed diagnostic testing has the potential to dramatically improve the quality of healthcare. Simultaneous measurement of health indicators and/or disease markers reduces turnaround time and analysis cost and speeds up the decision making process for diagnosis and treatment. At present, however, most diagnostic tests only provide information on a single indicator or marker. Development of efficient diagnostic tests capable of parallel screening of infectious disease markers could significantly advance clinical and diagnostic testing in both developed and developing parts of the world. Here, we report the multiplexed detection of nucleic acids as disease markers within discrete wells of a microfluidic chip using molecular beacons and total internal reflection fluorescence microscopy (TIRFM). Using a 4 × 4 array of 200 pL wells, we screened for the presence of four target single stranded oligonucleotides encoding for conserved regions of the genomes of four common viruses: human immunodeficiency virus-1 (HIV-1), human papillomavirus (HPV), Hepatitis A (Hep A) and Hepatitis B (Hep B). Target oligonucleotides are accurately detected and discriminated against alternative oligonucleotides with different sequences. This combinatorial chip represents a versatile platform for the development of clinical diagnostic tests for simultaneous screening, detection and monitoring of a wide range of biological markers of disease and health using minimal sample size.

Introduction

Rapid and efficient clinical assays based on integrated microdevices have the potential to revolutionize medical diagnosis and treatment.[1–9] Microfluidic approaches offer several key advantages for diagnostic applications, including miniaturized instrumentation, reduced amounts of sample and reagents for analysis, and integration of assay steps such as sample preparation (processing of physiological fluids), post-processing (*e.g.* reagent mixing, labeling, separation), detection and analysis into a single device. Miniaturization often improves detection sensitivity and facilitates portability for remote or point-of-care diagnostics. Capitalizing on these advantages, a variety of microfluidic-based diagnostic devices have been developed to perform assays in lab-on-a-chip format for detecting, diagnosing and monitoring disease.[10–19]

Accurate diagnosis often requires multiple clinical tests for a number of health or disease indicators. Due to small sample/reagent volumes, integration, and miniaturization, microfluidic methods enable the development of multiplexed assays to facilitate parallel screening and detection. Therefore, multiplexed microfluidic devices have the potential to accelerate diagnosis by simultaneously measuring multiple indicators of a single disease or by screening and detecting markers of several diseases using small amounts of sample (*e.g.* a drop of blood).[20–25] In this work, we report a combinatorial microfluidic approach for the detection of nucleic acid fragments as markers of infectious disease.

Viral genomes are an important class of molecular markers for infectious disease. Distinct classes of viral genomes consist of single-stranded DNA (ssDNA) or single-stranded RNA (ssRNA), and detection of this nucleic acid content is critical for identifying and diagnosing viral infections. To this end, genomic DNA or mRNA product markers produced during viral infection can be directly detected using Southern or Northern blotting methods, respectively. In addition, flow cytometry,[26] RT-PCR,[27,28] microcantilever-based biosensing,[29] and ELISA[30] have been used in assay techniques to screen for viral markers. Although these methods can accurately determine the identity of a particular virus, simultaneous screening for multiple infectious species with broad genetic diversity and/or detection of mutant strains of a specific virus is often cumbersome, time-consuming and costly.

[a]*Chemical & Biomolecular Engineering, University of Illinois at Urbana-Champaign, 600 South Matthews Avenue, Urbana, IL, USA. E-mail: kenis@illinois.edu; Tel: +1 (217) 265 0523; cms@illinois.edu; +1 (217) 333 3906*
[b]*Center for Biophysics and Computational Biology, University of Illinois at Urbana-Champaign, Urbana, IL, USA*
[c]*Center for Nanoscale Chemical Electrical Mechanical Manufacturing Systems, University of Illinois at Urbana-Champaign, Urbana, IL, USA*
† Electronic supplementary information (ESI) available. See DOI: 10.1039/c0lc00342e

Molecular beacons provide a promising approach for sensitive detection of single stranded nucleic acids (ssDNA, ssRNA) due to the intrinsic adaptability for multiplexing using small sample sizes. Molecular beacons are fluorescence-based reporters of unlabelled nucleic acids with sensitivity and sequence specificity comparable to standard laboratory techniques such as restriction fragment digestion analysis. The ability to engineer the sequence of the probe region of molecular beacons (see Materials and methods) allows for sequence specific detection of distinct nucleic acids, and in particular, accurate discrimination of "target" sequences in the presence of nucleic acids with only a single base mismatch.[31–35] Recognition of single nucleotide variations enables discrimination between alleles[32,33] and detection of point mutations,[34,35] thereby facilitating screening and detection of mutant strains of infectious viruses or bacteria (*e.g. Mycobacterium tuberculosis*).[36,37] Therefore, a nucleic acid detection assay based on molecular beacons coupled with a combinatorial microfluidic approach would enable large-scale multiplexing to simultaneously screen for a diverse set of genomic markers of viral infection in a single experiment using small sample sizes (microlitre to nanolitre volumes).

Here, we present a microfluidic method for screening and detection of multiple target oligonucleotides encoding for conserved genomic regions of several common viruses using molecular beacons (Fig. 1). Hybridization of a target oligonucleotide to its surface-immobilized complementary molecular beacon probe is detected using total internal reflection fluorescence microscopy (TIRFM). The microfluidic chip features a previously reported 4 × 4 array of microwells,[38] which facilitates the multiplexed detection of nucleic acid markers (ssDNA/ssRNA) for different diseases. The microfluidic chip enables quick (<2 hours) and simultaneous screening and detection of 16 different infectious disease markers using small amount of sample (3 μL) and reagents (pico to nanograms). The method outlined here can be implemented in rapid screening of a wide variety of health/disease indicators for faster, cost-effective diagnosis.

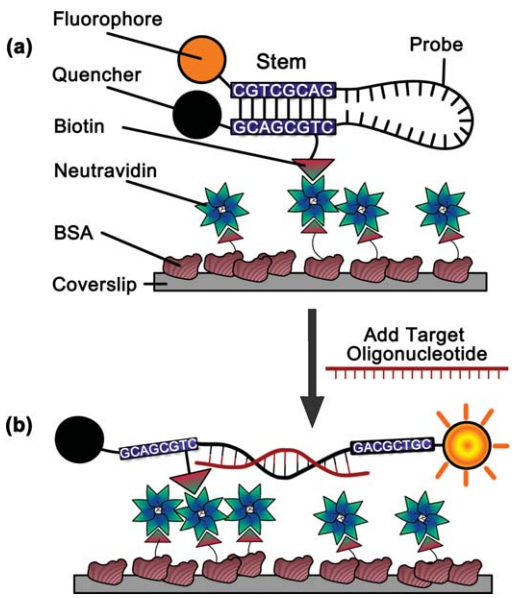

Fig. 1 Schematic of nucleic acid detection using molecular beacons. (a) At room temperature, molecular beacons exist in a hairpin configuration due to self-hybridization of the stem, which consists of eight complementary base pairs (quenched state, top). (b) The molecular beacon hairpin (closed state) converts to an extended conformation (open state) upon hybridization with its complementary target oligonucleotide (fluorescent state, bottom). Beacons are surface immobilized using neutravidin–biotin linkage.

Materials and methods

Design and immobilization of molecular beacons

Molecular beacons are single stranded oligonucleotide probes with a hairpin structure consisting of a "probe" region, a "stem" region, and a fluorophore/quencher pair covalently attached to the 5′ and 3′ termini of the molecular beacon, respectively.[31] The "probe" region consists of a single stranded DNA loop and is designed to contain the complementary sequence of an intended "target" oligonucleotide. The beacon stem consists of 5–8 self-complementary base pairs at the 5′ and 3′ termini of the oligonucleotide. Molecular beacons are designed to remain folded in a hairpin structure at room temperature by self-hybridization of the stem (Fig. 1a). In the hairpin configuration, the fluorophore and the quencher are in close proximity, and fluorescence emission from the fluorophore is suppressed by the quencher. Upon hybridization of the target oligonucleotide to the probe sequence, the molecular beacon converts to an open conformation, thereby separating the quencher and fluorophore pair by several nanometres which results in fluorescence emission from the molecular beacon (Fig. 1b). In this work, molecular beacons are designed to detect different 20-base target oligonucleotides corresponding to the conserved regions of four distinct viral genomes, specifically: human immunodeficiency virus-1 (HIV), human papillomavirus (HPV), Hepatitis A (Hep A) and Hepatitis B (Hep B).[39–42] We used a universal 8-base pair stem covalently functionalized with a fluorescence quencher (Iowa Black) and hexachlorofluorescein (HEX) on the 3′ and 5′ termini, respectively. A single nucleotide near the 3′ terminus in the stem is biotinylated, which facilitates surface immobilization through a biotin–Neutravidin linkage. To optimize oligonucleotide detection, we systematically investigated several design parameters for the molecular beacons used in this study, including the beacon stem length, the location of

Table 1 DNA sequences of the target viral nucleic acid markers (single stranded oligonucleotides) and the corresponding molecular beacons, including the stem region. All sequences are shown in the 5′ to 3′ orientation

Targets (conserved viral DNA sequences)	
cHIV 5′	GGCGAGGGGCGGCGACTGGTGAGTA
cHPV 5′	CTGACACCTTTGGCACAACTGGTTTT
cHep A 5′	CCGCCGCTGTTACCCTATCC
cHep B 5′	CATCCATATAACTGAAAGCC
Probes (embedded in molecular beacons)	
HIV	#TACTCACCAGTCGCCGCCCCTCGCC$
HPV	#AAAACCAGTTGTGCCAAAGGTGTCAGC$
Hep A	#GGATAGGGTAACAGCGGCGGC$
Hep B	#GGCTTTCAGTTATATGGATGC$
Stem	
#: 5′ universal stem, 5′ hexachlorofluorescein/CGTCGCAG	
$: 3′ universal stem, 5′ C/T*/GCGACG/Iowa Black/3′	
T*: biotinylated nucleotide	

the biotin moiety along the stem and the fluorophore/quencher pair (see ESI†). Overall, the sequences of the probes, targets, and the stem listed in Table 1 yielded the best conditions for surface immobilization and target oligonucleotide detection by fluorescence. All molecular beacons and target oligonucleotides were purchased from Integrated DNA Technologies (IDT) and used without further purification.

Molecular beacons were immobilized on the exposed glass surfaces within the wells of the microfluidic device *via* Neutravidin–biotin interaction (Fig. 1). The glass surfaces are sequentially incubated with Bovine Serum Albumin (BSA)–biotin, Neutravidin, and biotinylated molecular beacons, thereby resulting in surface-immobilized molecular beacons within the microwells (Fig. 1). The protocol consists of four sequential steps performed at room temperature: (a) BSA–biotin [1.0 mg mL^{-1}] incubated for 10 minutes; (b) Neutravidin [0.5 mg mL^{-1}] incubated for 10 minutes; (c) BSA [2.0 mg mL^{-1}] as a surface blocking agent to minimize non-specific adsorption, incubated for 10 minutes; and (d) biotinylated molecular beacons incubated for 10 minutes at various concentrations. Between each step, wells were rinsed with TE50 buffer (50 mM Tris/Tris–HCl, 10 mM NaCl, 1 mM EDTA, pH 8.0).

Fluorescence measurements using TIRF microscopy

We used objective-type total internal reflection fluorescence microscopy (TIRFM)[43] to measure the fluorescence signal from the molecular beacons upon hybridization with target oligonucleotides. TIRFM allows for selective illumination and excitation of fluorophores within close proximity (<100–200 nm) to the glass coverslip surface. Confinement of the illumination near the surface effectively reduces background fluorescence from solution or PDMS walls and enables high sensitivity measurements. An inverted microscope (Olympus, IX71) with a high numerical aperture objective lens (100×, NA = 1.40) interfaced with an EMCCD camera (Andor iXon+) was used for detection, and a CW green laser (532 nm, CrystaLaser) was used for illumination. A dichroic mirror (Chroma, z532rdc) and an emission filter (Chroma, 550LP) were used to collect the fluorescence emission from the molecular beacons.

Design and operation of the microfluidic screening chip

The microfluidic chip used in this study consists of a 4 × 4 array of wells, which is a highly effective design that was utilized previously in a "label-free" protein binding assay (Fig. 2).[38] Each array element is approximately 1 × 1 mm (yielding a 4 × 4 mm chip) and consists of two half-wells and three sets of valves to control fluid flow and facilitate mixing. Effective channel dimensions for the half-wells are 100 μm (width) and 20 μm (height). The microfluidic device consists of a fluidic layer and a pneumatic control layer fabricated using polydimethylsiloxane (PDMS)-based multilayer soft lithography and replica molding.[44] After device fabrication, the monolithic PDMS structure is placed on a glass coverslip to seal the fluidic compartments and to facilitate imaging within the channels using optical microscopy.

Within the array, individual wells are comprised of two half-wells, each with a volume of 200 picolitres. Using this strategy,

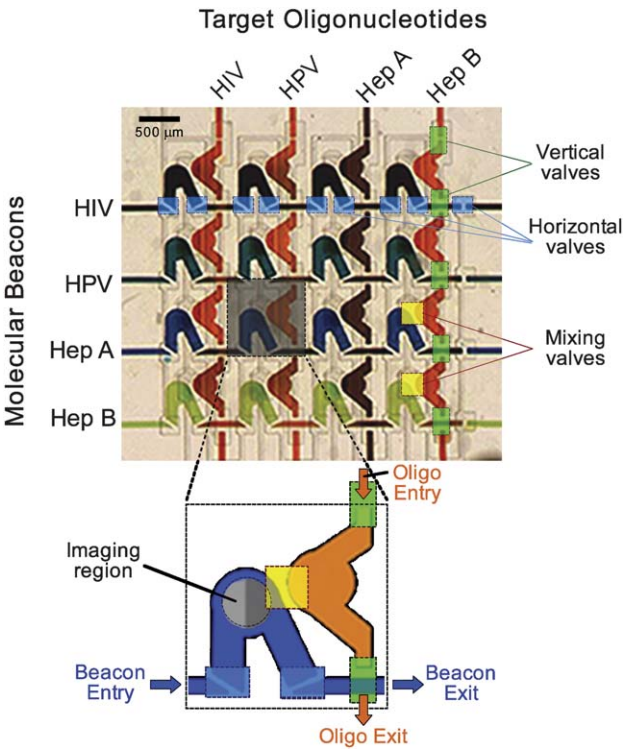

Fig. 2 Optical micrograph of the microfluidic screening chip, filled with dye solutions indicating its combinatorial capabilities. The 4 × 4 array is comprised of 16 sets of two 200 pL sized half-wells. Fluid access to the wells is controlled by two sets of individually addressable valves in the horizontal (blue boxes) and vertical (green boxes) direction. Mixing between the adjacent half wells is initiated by a separate set of valves (yellow boxes). Molecular beacons and complementary target oligonucleotides are introduced *via* the rows and columns, respectively. The inset shows a schematic view of a pair of half-wells with the corresponding valves. Fluorescence images are acquired in the half well initially containing the molecular beacons. The regions of interest for background and signal detection are shown in light and dark gray, respectively.

four rows and four columns of half-wells can be independently addressed and filled with liquid. In addition, the device has a set of mixing valves, which allows for mixing within adjacent half-wells after rows and columns are loaded with fluid. Using this device, 4 × 4 = 16 different combinations of chemistries can be screened in an "on-chip" format.

The device has three sets of independent valves: one set to open horizontal fluid lines (rows); one set to open vertical fluid lines (columns); and one set to mix the contents of adjacent sets of two-half-wells (Fig. 2). Valves are designed to be closed in the rest state (*i.e.* referred to as actuate-to-open valves in prior work[38]) and are used to isolate various compartments in the chip. Valves are actuated (opened) by applying a negative gauge pressure of −600 Torr to the appropriate pneumatic line in the control layer. In addition, sample is loaded into the half-wells by applying vacuum on the device.

To fill a specific row or a column of half-wells with solution, a 3 μL droplet of reagent is placed at the corresponding inlet and drawn into the device by applying vacuum to the exit port while opening the corresponding valves.

In this work, we immobilize four different molecular beacons in the four rows of half-wells, while samples containing target oligonucleotides are introduced through the four columns of half-wells (Fig. 2). Opening the set of valves between adjacent half-wells allows the target oligonucleotides to interact and bind with the immobilized molecular beacons for detection. Repeated actuation of the mixing valves increases the rate of oligonucleotide hybridization within each solution.

Results and discussion

Characterization of molecular beacons

To characterize the properties of molecular beacon binding to target oligonucleotides, we determined the sensitivity limit of molecular beacon-based oligonucleotide detection (Fig. 3a), the bulk-phase binding kinetics of a target oligonucleotide to a specific molecular beacon (Fig. 3b), and the effect of surface immobilization of molecular beacons on target binding and fluorescence detection (Fig. 3c).

The sensitivity limit of oligonucleotide detection by molecular beacons was determined through a bulk experiment (using 50–200 μL of sample in each well) performed using a 96-well microplate reader (Tecan Safire^2, Switzerland). Individual wells were filled with solution containing the molecular beacon specific for HIV-1 viral genetic material at increasing concentrations (Fig. 3a). In this experiment, the molecular beacons were in free solution (not surface-immobilized). The corresponding target oligonucleotide, cHIV, was added to each well in a series of concentrations spanning the lower end of the detectable range (0–250 nM). Molecular beacon–oligonucleotide complexes were allowed to hybridize at room temperature for 1 hour, followed by measurement of fluorescence emission in each well. As shown in Fig. 3a, molecular beacons exhibit background fluorescence even in the absence of the target oligonucleotide, presumably arising from ill-formed hairpins, which disrupt quencher–dye pairs. The minimum oligonucleotide concentration resulting in a fluorescence signal distinguishable from the background was approximately 10 nM. Therefore, we determined the detection sensitivity limit as ~10 nM for target oligonucleotides, which is comparable to previously reported values.[31] In addition, the oligo hybridization kinetic measurements at low oligonucleotide concentrations (10 nM) also support the observed detection sensitivity limit (see below).

Next, we characterized the hybridization kinetics of a target oligonucleotide to its corresponding molecular beacon. In bulk-phase experiments using a microplate reader, solution mixing is readily achieved by agitation or other inertially driven fluid flow. However, mixing over small length scales in a microfluidic compartment occurs primarily due to diffusion. In the on-chip combinatorial screening experiment, the minimum time for fluorescence measurements is determined by the slower of either the bulk hybridization rate or the on-chip diffusional mixing rate. To determine the minimum time needed for full beacon–oligo hybridization, we measured bulk-phase hybridization kinetics between a molecular beacon and its target oligonucleotide in the absence of any diffusion limitations using a microplate reader. Molecular beacons for detecting HIV-specific oligonucleotide were introduced into four wells of a microplate at 250 nM,

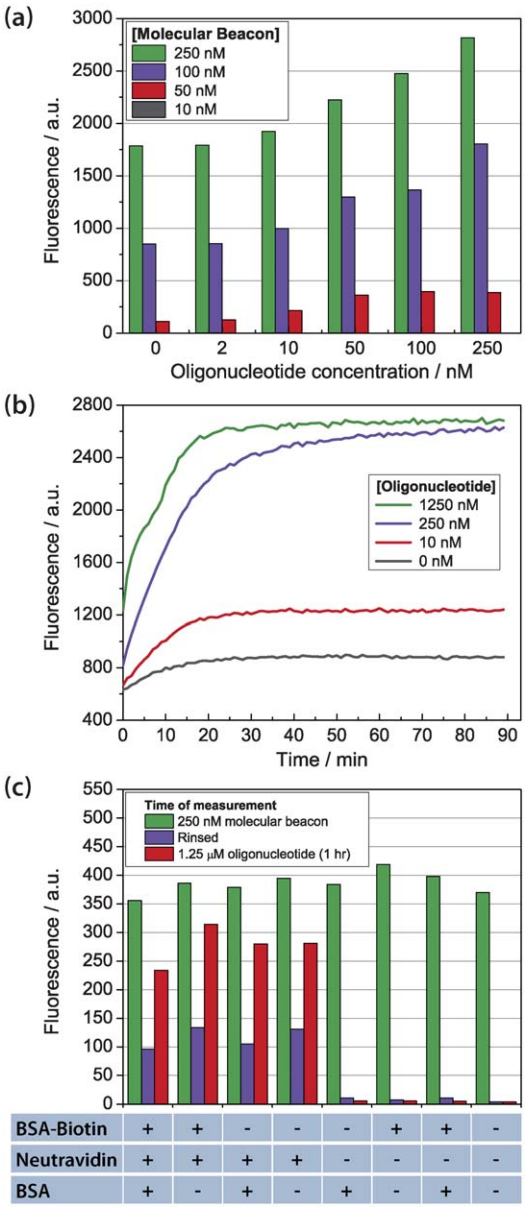

Fig. 3 Bulk-phase molecular beacon characterization experiments. (a) Sensitivity limit determination of target oligonucleotide detection. Four concentrations of the HIV-1 molecular beacon (10 nM, 50 nM, 250 nM and 500 nM) were assayed against six concentrations of its complementary target oligonucleotide cHIV (0, 2 nM, 10 nM, 50 nM, 100 nM and 250 nM). (b) Hybridization kinetics of molecular beacons (250 nM) with target oligonucleotides (four concentrations: 0, 10, 250, 1250 nM). (c) Establishing appropriate protocol for surface immobilization of molecular beacons. The table at the bottom specifies the different surface treatments tested. Fluorescence detection was performed at three time points: after incubation with 250 nM molecular beacon (green), after rinsing the beacon solution with TE50 buffer (purple), and 1 hour after the introduction of the complementary target oligonucleotide (red).

followed by addition and thorough mixing of four different concentrations of target oligonucleotide (cHIV) at time zero. Fluorescence emission was monitored for 90 minutes (Fig. 3b). The fluorescence signal reached a plateau within 20 minutes, which is much greater than the diffusive mixing timescale within the microfluidic wells used here ($t_{diff} \approx 250$ seconds (4 minutes)

assuming $D_{oligo} \approx 1 \times 10^{-7}$ cm^2 s^{-1} for oligonucleotides diffusing over a distance of ~100 μm). Therefore, the limiting step in oligonucleotide detection using our microfluidic-based method is beacon–oligo hybridization suggesting that the on-chip assay is not impeded by prolonged diffusional mixing. It should be noted that the initial fluorescence measurements ($t = 0$) for each nucleotide concentration are different because the initial measurement is performed after the addition and mixing of the oligonucleotides. The increase in background signal (0 nM oligonucleotide) is due to slow degradation of the molecular beacons, *i.e.*, opening of hairpins or disruption of efficient dye quenching.

In the combinatorial screening chip, molecular beacons are attached to the surface *via* Neutravidin–biotin interaction as shown in Fig. 1. In order to maximize surface coverage and minimize background fluorescence signal, we characterized the effect of different surface treatments on the immobilization efficiency of biotinylated molecular beacons to the surface in a 96-well plate (Fig. 3c). We examined the efficacy of the three surface modification steps (BSA–biotin, Neutravidin and BSA) on molecular beacon function and fluorescence by considering combinations (8 total) that included (+) or excluded (−) a surface modification step (Fig. 3c). For each set of surface treatments, fluorescence was measured at three time points: (1) after incubation with 250 nM of HIV-1 molecular beacon, ('250 nM molecular beacon', Fig. 3c), such that molecular beacons are both surface bound and in free-solution; (2) after rinsing with TE50 buffer ('Rinsed', Fig. 3c); and (3) 1 hour after addition of 1.25 μM of the matching target oligonucleotide cHIV ('1.25 μM oligonucleotide (1 hour)', Fig. 3c). The results show that the critical step in surface immobilization of molecular beacons is the binding of Neutravidin to the surface, which facilitates tethering of the biotinylated molecular beacons to the glass surface. The resulting signal-to-noise ratios for molecular beacons (hybridized with the target oligonucleotide) immobilized to the surface *via* Neutravidin treatment suggest that the highest signal-to-noise ratio can be obtained from a Neutravidin treatment preceded by a BSA–biotin treatment step. However, we followed standard surface immobilization protocols for TIRF-based assays which include BSA as a surface passivation agent. With further development, assays performed in our combinatorial screening chip may be extended to include other biological components (additional DNA/RNA/proteins), and the addition of BSA will likely be required to passivate the chip components in order to suppress background fluorescence. Therefore, although steps (a) and (c) appear to be less essential, all three surface modification steps were utilized to immobilize molecular beacons and to minimize background fluorescence in the microfluidic chip.

The total assay time can be reduced by shortening the surface modification steps as well as the incubation step. For example, the final surface treatment step with BSA can be omitted without compromising detection sensitivity. In addition, the incubation time can be reduced to 20 minutes as the fluorescence signal upon molecular beacon–target oligonucleotide hybridization reaches to a steady-state value within 20 minutes.

On-chip viral nucleic acid marker screening experiment

We used the 4 × 4 microfluidic array chip shown in Fig. 2 for sequence-specific detection of oligonucleotides encoding for conserved regions of the genomes of four common viruses using surface immobilized molecular beacons and TIRF microscopy. First, molecular beacons were immobilized on the microwell surfaces. Next, target oligonucleotides were introduced into the microwells and mixed with the molecular beacons to allow for hybridization. Finally, fluorescence arising from successful beacon–oligo (probe–target) hybridization was detected using TIRF microscopy.

We immobilized four molecular beacons (HIV-1, HPV, Hep A, Hep B, see Table 1) on the glass surface in four rows of half-wells of the 4 × 4 combinatorial screening chip. First, BSA–biotin, Neutravidin, and BSA were introduced successively to all rows of half-wells according to the surface functionalization protocol specified above. Next, solutions containing the four molecular beacons (250 nM) were introduced to successive rows and incubated for 1 hour. After rinsing away unbound molecular beacons, the chip was ready for screening of oligonucleotide binding by fluorescence microscopy.

To demonstrate the capability of the combinatorial chip to detect the presence of target oligonucleotides, solutions containing the four complementary oligonucleotides (1.25 μM) were introduced to successive columns of half-wells. After loading the device, the sets of valves connecting the two adjacent half-wells were opened and closed repeatedly (once per minute for 10 minutes) to initiate and accelerate mixing of the solutions, thereby introducing the immobilized molecular beacons to the target oligonucleotide solution.

To detect for hybridized molecular beacon–target oligonucleotide complexes, fluorescence measurements were performed using TIRF microscopy within the half-wells containing the surface immobilized molecular beacons (see ESI† for details on image acquisition, data analysis and statistical methods). Data were collected by capturing 100 successive images of three different spots (regions of interest, ROIs) within each of the 16 half-wells. Using a different ROI for each measurement minimizes the effects of photobleaching. The ROIs were selected to be located far from the PDMS microchannel walls to avoid excessive background fluorescence. The intensity measurement for the background and fluorescence signal was obtained by calculating the mean pixel intensity value for 100 successive images of each ROI. To determine the background signal, we imaged the surface-immobilized molecular beacons in each of the 16 half-wells prior to mixing with target oligonucleotides. Fluorescence signal was then measured in each well following the introduction and incubation of the four corresponding target oligonucleotides. The net fluorescence response was determined by subtracting the background signal from the fluorescence signal obtained from the molecular beacon–target complexes. To minimize photobleaching, the background signal measurements were performed only on the left side of the half-well (light gray), whereas fluorescence signal measurements were performed on the right side (dark gray) of the same half-well (see inset Fig. 2).

The results of the combinatorial on-chip viral nucleic acid marker detection experiment are shown in Fig. 4. The experiment was designed such that matches between molecular beacon and target oligonucleotide would be expected along the diagonal of the 4 × 4 array. Indeed, the screening chip accurately detects positive matches in a sequence-specific manner. The fluorescence

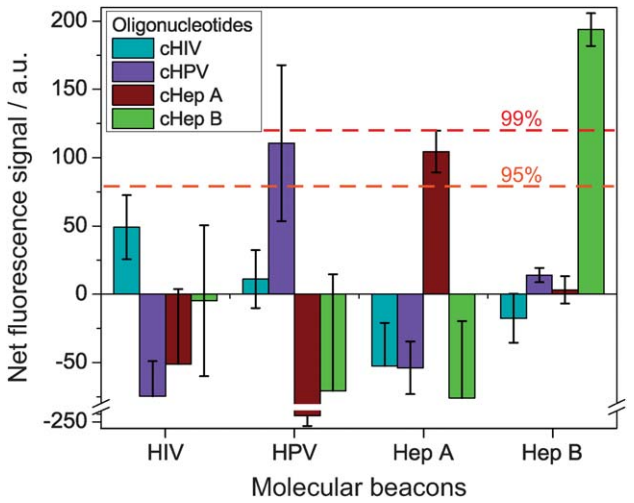

Fig. 4 On-chip screening of oligonucleotides encoding for viral genomic content. Four molecular beacons are tested in a combinatorial fashion in their ability to detect and identify the presence of four complementary target oligonucleotides. For each molecular beacon (*x*-axis), only the matching target oligonucleotide showed a statistically significant positive signal. Dashed lines: upper limits of statistical confidence levels (*z*-test).

response of the matching combinations of molecular beacons and target viral oligonucleotides (HIV–cHIV, HPV–cHPV, *etc.*) far exceeds the fluorescence response of the mismatched pairs. For each molecular beacon, only the matching target oligonucleotide showed a statistically significant positive signal. The average fluorescence intensity for the four molecular beacon–oligonucleotide binding events and the twelve mismatch (non-binding) events are 114.47 ± 59.69 (mean $\pm$ standard error of the mean (SEM), $N = 4$) and -50.22 ± 65.99 ($N = 12$), respectively, where values represent fluorescence signal with background values subtracted. A net average fluorescence intensity value of 164.69 corresponds to a *z*-value of 2.495 and represents the upper limit of 98.74% confidence interval. The upper limits for the 95% and 99% confidence intervals are shown in Fig. 4. The signal-to-noise ratios (SNR) for each detection event are as follows: $SNR_{HIV} = 1.12$, $SNR_{HPV} = 1.81$, $SNR_{HEP\ A} = 1.74$, $SNR_{HEP\ B} = 2.74$. The coefficient of variation between the measurements for the four positive binding events is 0.52 suggesting a relatively small dispersion between the assays performed in the microfluidic device.

In a few mismatch cases (*e.g.*, HPV–cHep A), a large negative signal was detected, which presumably arises due to a high background fluorescence signal in one of the ROIs within the microchannel well. Such behavior can be circumvented by using more ROIs, minimizing intensity fluctuations across the ROIs by eliminating inhomogeneities in surface treatment, and/or using threshold criteria to exclude aberrant measurements.

We repeated the on-chip viral nucleic acid marker screening experiments at lower molecular beacon/target oligonucleotide concentrations (100 pM/100 nM respectively, see the ESI†) and successfully detected/identified the presence of four target oligonucleotides with similar statistical significance as the results shown in Fig. 4. In both experiments, we observed fluctuations in the fluorescence and background signals corresponding to positive (binding) and negative (non-binding) detection of molecular beacon–target oligonucleotide hybridization. The fluctuations in fluorescence and background signals might arise due to potential issues in performing the assay: (i) variability in surface properties during the surface immobilization protocol; (ii) irregularities in microfluidic wells that might impact fluorescence measurements such as adsorbed impurities; (iii) optimal design and sequence-dependence of molecular beacons. For full-scale clinical applications, additional optimization studies are needed to identify the sources of noise and improve the signal-to-noise ratio. However, in this work, our data represent proof-of-principle validation of the general approach.

Statistical significance testing for the determination of nucleic acid detection events

Statistical hypothesis testing is employed to discriminate between the nucleic acid detection events (molecular beacon–target oligonucleotide binding events) and the mismatch (non-binding) events. In particular, we performed a Wilcoxon test, which is a non-parametric test that estimates the significance of a positive measurement being a true hit as opposed to occurring by chance. The Wilcoxon test has been widely applied for hypothesis testing in pathogen detection in clinical isolates,[45] comparing real time PCR data[46] and in bioinformatics sequence alignments.[47]

Initially, we applied the Wilcoxon Rank test to the raw experimental data for each type of viral nucleic acid marker comparing the fluorescence signal from the positive events (oligonucleotide binding/detection) with the average of the fluorescence signal from the negative (non-binding) events. The *p*-value obtained for the detection events was reasonably low (=0.0286) confirming that the "hits" could not have arisen by mere chance alone and represented actual molecular beacon–target oligonucleotide binding events.

Statistical significance tests provide more reliable results when the sample size increases.[48] We obtained larger datasets ($N \geq 10$) by resampling the experimental data for each of the four nucleic acids. Specifically, we resampled the positive (binding) events from a normal distribution (with mean and variance equal to that of the original dataset) and negative (non-binding) events by bootstrapping.[49] Then, we applied the Wilcoxon Rank test to each of these four larger datasets, comparing the positive and the negative events and reporting the *p*-value estimate for each of the four viral nucleic acid markers. The actual *p*-values ($p_{HIV} = 1.766 \times 10^{-4}$, $p_{HPV} = 1.485 \times 10^{-4}$, $p_{HEP\ A} = 1.707 \times 10^{-4}$, $p_{HEP\ B} = 1.766 \times 10^{-4}$) were significantly low, confirming the conclusions from the smaller dataset. The statistical testing method outlined here facilitates the discrimination of detection events from a limited dataset.

Conclusion

In this work, we report a combinatorial screening chip for high sensitivity, sequence-specific and multiplexed detection of viral nucleic acid markers (ssDNA) using surface immobilized molecular beacons and TIRF microscopy. The chip features a 4×4 array of 200 pL microwells configured to enable screening of minute amounts of sample in a multiplexed fashion. We demonstrated successful on-chip screening and detection of four target oligonucleotides encoding for conserved regions of the

genomes of four common viruses, specifically human immunodeficiency virus-1 (HIV), human papillomavirus (HPV), Hepatitis A (Hep A) and Hepatitis B (Hep B). These target oligonucleotide sequences are accurately discriminated against oligonucleotides with alternative sequences.

Here, we demonstrate a proof-of-concept microdevice for multiplexed detection of target oligonucleotides as markers of infectious disease. With additional development, sample preparation methods to isolate, purify and amplify nucleic acids may be integrated directly "on-chip",[50–52] which would enable the analysis and screening of clinical samples such as a drop of blood in an integrated diagnostic device. The small sample well volume (200 pL) in our microfluidic device results in a relatively small number of target molecules in each well ($\sim 1.2 \times 10^8$ molecules per well at 1 μM) which may necessitate a sensitive detection system for screening assays. Combined with TIRF microscopy, our combinatorial microfluidic chip has the potential to enable the detection of fluorescent samples at extremely low concentrations and to perform assays using minute amounts of sample without compromising detection sensitivity.

Surface immobilized molecular beacons serve as effective reporters for nucleic acids with high sensitivity and specificity, thereby enabling direct detection of unlabelled ssDNA and ssRNA. The sequence of the probe region can be engineered providing flexibility in screening for a wide variety of nucleic acid markers associated with different diseases in a multiplexed fashion. For instance, the combinatorial microfluidic chip described in this work could be used to perform a simple diagnostic assay to detect single nucleotide polymorphisms (SNPs) for individual genotype analysis for personalized medicine.[53]

In addition, the combinatorial microfluidic chip could also be utilized in screening and detecting DNA–protein interactions in a multiplexed fashion to develop diagnostic tools for basic and applied biosciences. For example, molecular beacon and aptamer based detection technologies have been applied to detect DNA binding proteins[54–57] (*e.g.* single-stranded DNA binding protein) and cleavage products of restriction endonucleases.[58]

Furthermore, although we used nucleic acid detection as proof-of-principle demonstration of disease marker screening in this work, a diverse set of alternative disease diagnostic methods including, but not limited to, antibody recognition (immunoassays, ELISA) and chemical (small molecule) marker detection can be employed with our microfluidic chip.

Fluorescence-based techniques are well-suited for multiplexed detection applications. Simultaneous measurement of multiple biological samples increases throughput and subjects all screens to a standardized set of conditions such that measurements are performed using the same set of stock solutions and on the same day using identical conditions. In this way, simultaneous measurements as enabled by the combinatorial chip serve as an internal control for systematic or random human error. In our experiment, surface-immobilized molecular beacons coupled with TIRF microscopy facilitate accurate detection of nucleic acids. By employing on-chip optimization and calibration procedures, it may be possible to perform quantitative screening assays at high sensitivity limits for molecular beacons as shown in Fig. 3.

Microfluidic chips with multiplexing capabilities, such as those reported here, have the potential to serve as an effective means for simultaneous screening, detecting and monitoring of a wide range of disease indicators such as metabolic, endocrine or cardiac markers, allergens, cytokines, and cancer markers in a single experiment using minute amounts of sample. Therefore, our microfluidic chip could serve as a valuable diagnostic tool in a clinical laboratory when coupled with a fluorescence detection system, as described in this work. In addition, at the expense of sensitivity, a less-complicated detection scheme (*e.g.* a handheld fluorescence reader) could be developed to provide portability for point-of-care diagnostics.

Acknowledgements

This work was performed within Nano-CEMMS, a Nano-Science and Engineering Center (NSEC) at the University of Illinois Urbana-Champaign, supported by the National Science Foundation under awards DMI 0328162 and CMMI 0749028. C.M.S. acknowledges funding by an NIH Pathway to Independence PI Award 4R00HG004183-03.

References

1 P. Yager, T. Edwards, E. Fu, K. Helton, K. Nelson, M. R. Tam and B. H. Weigl, *Nature*, 2006, **442**, 412–418.
2 C. D. Chin, V. Linder and S. K. Sia, *Lab Chip*, 2007, **7**, 41–57.
3 P. Yager, G. J. Domingo and J. Gerdes, *Annu. Rev. Biomed. Eng.*, 2008, **10**, 107–144.
4 W. G. Lee, Y. G. Kim, B. G. Chung, U. Demirci and A. Khademhosseini, *Adv. Drug Delivery Rev.*, 2010, **62**, 449–457.
5 J. Hong, J. B. Edel and A. J. deMello, *Drug Discovery Today*, 2009, **14**, 134–146.
6 L. F. Kang, B. G. Chung, R. Langer and A. Khademhosseini, *Drug Discovery Today*, 2008, **13**, 1–13.
7 B. Weigl, G. Domingo, P. LaBarre and J. Gerlach, *Lab Chip*, 2008, **8**, 1999–2014.
8 A. M. Dupuy, S. Lehmann and J. P. Cristol, *Clin. Chem. Lab. Med.*, 2005, **43**, 1291–1302.
9 C. P. Price, *Br. Med. J.*, 2001, **322**, 1285–1288.
10 E. T. Lagally, J. R. Scherer, R. G. Blazej, N. M. Toriello, B. A. Diep, M. Ramchandani, G. F. Sensabaugh, L. W. Riley and R. A. Mathies, *Anal. Chem.*, 2004, **76**, 3162–3170.
11 V. Srinivasan, V. K. Pamula and R. B. Fair, *Lab Chip*, 2004, **4**, 310–315.
12 M. Toner and D. Irimia, *Annu. Rev. Biomed. Eng.*, 2005, **7**, 77–103.
13 A. E. Herr, A. V. Hatch, D. J. Throckmorton, H. M. Tran, J. S. Brennan, W. V. Giannobile and A. K. Singh, *Proc. Natl. Acad. Sci. U. S. A.*, 2007, **104**, 5268–5273.
14 J. M. Klostranec, Q. Xiang, G. A. Farcas, J. A. Lee, A. Rhee, E. I. Lafferty, S. D. Perrault, K. C. Kain and W. C. W. Chan, *Nano Lett.*, 2007, **7**, 2812–2818.
15 R. Fan, O. Vermesh, A. Srivastava, B. K. H. Yen, L. D. Qin, H. Ahmad, G. A. Kwong, C. C. Liu, J. Gould, L. Hood and J. R. Heath, *Nat. Biotechnol.*, 2008, **26**, 1373–1378.
16 R. J. Meagher, A. V. Hatch, R. F. Renzi and A. K. Singh, *Lab Chip*, 2008, **8**, 2046–2053.
17 M. A. Alyassin, S. Moon, H. O. Keles, F. Manzur, R. L. Lin, E. Haeggstrom, D. R. Kuritzkes and U. Demirci, *Lab Chip*, 2009, **9**, 3364–3369.
18 L. Gervais and E. Delamarche, *Lab Chip*, 2009, **9**, 3330–3337.
19 M. Hu, J. Yan, Y. He, H. T. Lu, L. X. Weng, S. P. Song, C. H. Fan and L. H. Wang, *ACS Nano*, 2010, **4**, 488–494.
20 D. Gruson and S. Bodovitz, *Biomarkers*, 2010, **15**, 289–296.
21 Y. G. Li, Y. T. H. Cu and D. Luo, *Nat. Biotechnol.*, 2005, **23**, 885–889.
22 A. M. Smith, S. Dave, S. M. Nie, L. True and X. H. Gao, *Expert Rev. Mol. Diagn.*, 2006, **6**, 231–244.
23 A. Zajac, D. S. Song, W. Qian and T. Zhukov, *Colloids Surf., B*, 2007, **58**, 309–314.
24 C. X. Lin, Y. Liu and H. Yan, *Nano Lett.*, 2007, **7**, 507–512.

25 D. C. Pregibon, M. Toner and P. S. Doyle, *Science*, 2007, **315**, 1393–1396.
26 C. P. Brussaard, D. Marie and G. Bratbak, *J. Virol. Methods*, 2000, **85**, 175–182.
27 M. Abbaszadegan, P. Stewart and M. LeChevallier, *Appl. Environ. Microbiol.*, 1999, **65**, 444–449.
28 K. M. Weinberger, E. Wiedenmann, S. Bohm and W. Jilg, *J. Virol. Methods*, 2000, **85**, 75–82.
29 T. Braun, M. K. Ghatkesar, N. Backmann, W. Grange, P. Boulanger, L. Letellier, H. P. Lang, A. Bietsch, C. Gerber and M. Hegner, *Nat. Nanotechnol.*, 2009, **4**, 179–185.
30 A. Voller, A. Bartlett, D. E. Bidwell, M. F. Clark and A. N. Adams, *J. Gen. Virol.*, 1976, **33**, 165–167.
31 S. Tyagi and F. R. Kramer, *Nat. Biotechnol.*, 1996, **14**, 303–308.
32 S. Tyagi, D. P. Bratu and F. R. Kramer, *Nat. Biotechnol.*, 1998, **16**, 49–53.
33 L. G. Kostrikis, S. Tyagi, M. M. Mhlanga, D. D. Ho and F. R. Kramer, *Science*, 1998, **279**, 1228–1229.
34 S. A. Marras, F. R. Kramer and S. Tyagi, *Genet. Anal.: Biomol. Eng.*, 1999, **14**, 151–156.
35 B. Dubertret, M. Calame and A. J. Libchaber, *Nat. Biotechnol.*, 2001, **19**, 365–370.
36 A. S. Piatek, S. Tyagi, A. C. Pol, A. Telenti, L. P. Miller, F. R. Kramer and D. Alland, *Nat. Biotechnol.*, 1998, **16**, 359–363.
37 A. M. Nascimento, G. H. Goldman, S. Park, S. A. E. Marras, G. Delmas, U. Oza, K. Lolans, M. N. Dudley, P. A. Mann and D. S. Perlin, *Antimicrob. Agents Chemother.*, 2003, **47**, 1719–1726.
38 B. R. Schudel, C. J. Choi, B. T. Cunningham and P. J. A. Kenis, *Lab Chip*, 2009, **9**, 1676–1680.
39 K. H. Abd El Galil, M. A. El Sokkary, S. M. Kheira, A. M. Salazar, M. V. Yates, W. Chen and A. Mulchandani, *Appl. Environ. Microbiol.*, 2004, **70**, 4371–4374.
40 S. D. Pas, S. Noppornpanth, A. A. van der Eijk, R. A. de Man and H. G. Niesters, *J. Clin. Virol.*, 2005, **32**, 166–172.
41 T. Takacs, C. Jeney, L. Kovacs, J. Mozes, M. Benczik and A. Sebe, *J. Virol. Methods*, 2008, **149**, 153–162.
42 J. A. Vet, A. R. Majithia, S. A. Marras, S. Tyagi, S. Dube, B. J. Poiesz and F. R. Kramer, *Proc. Natl. Acad. Sci. U. S. A.*, 1999, **96**, 6394–6399.
43 P. R. Selvin and T. Ha, *Single-Molecule Techniques: a Laboratory Manual*, Cold Spring Harbor Laboratory Press, Cold Spring Harbor, N.Y., 2008.
44 M. A. Unger, H. P. Chou, T. Thorsen, A. Scherer and S. R. Quake, *Science*, 2000, **288**, 113–116.
45 A. Davidow, G. V. Kanaujia, L. Shi, J. Kaviar, X. Guo, N. Sung, G. Kaplan, D. Menzies and M. L. Gennaro, *Infect. Immun.*, 2005, **73**, 6846–6851.
46 E. S. Bruijnesteijn van Coppenraet, J. A. Lindeboom, J. M. Prins, M. F. Peeters, E. C. J. Claas and E. J. Kuijper, *J. Clin. Microbiol.*, 2004, **42**, 2644–2650.
47 C. Notredame, D. G. Higgins and J. Heringa, *J. Mol. Biol.*, 2000, **302**, 205–217.
48 R. R. Sokal and F. J. Rohlf, *Biometry: the Principles and Practice of Statistics in Biological Research*, W.H. Freeman, New York, 1995.
49 A. R. Henderson, *Clin. Chim. Acta*, 2005, **359**, 1–26.
50 A. Bhattacharyya and C. M. Klapperich, *Anal. Chem.*, 2006, **78**, 788–792.
51 C. J. Easley, J. M. Karlinsey, J. M. Bienvenue, L. A. Legendre, M. G. Roper, S. H. Feldman, M. A. Hughes, E. L. Hewlett, T. J. Merkel, J. P. Ferrance and J. P. Landers, *Proc. Natl. Acad. Sci. U. S. A.*, 2006, **103**, 19272–19277.
52 J. Wen, L. A. Legendre, J. M. Bienvenue and J. P. Landers, *Anal. Chem.*, 2008, **80**, 6472–6479.
53 K. Abravaya, J. Huff, R. Marshall, B. Merchant, C. Mullen, G. Schneider and J. Robinson, *Clin. Chem. Lab. Med.*, 2003, **41**, 468–474.
54 T. Heyduk and E. Heyduk, *Nat. Biotechnol.*, 2002, **20**, 171–176.
55 H. Kuhn, V. V. Demidov, J. M. Coull, M. J. Fiandaca, B. D. Gildea and M. D. Frank-Kamenetskii, *J. Am. Chem. Soc.*, 2002, **124**, 1097–1103.
56 J. J. Li, X. Fang, S. M. Schuster and W. Tan, *Angew. Chem., Int. Ed.*, 2000, **39**, 1049–1052.
57 S. Zhang, V. Metelev, D. Tabatadze, P. C. Zamecnik and A. Bogdanov, *Proc. Natl. Acad. Sci. U. S. A.*, 2008, **105**, 4156–4161.
58 C. Ma, Z. Tang, K. Wang, W. Tan, X. Yang, W. Li, Z. Li and X. Lv, *Anal. Biochem.*, 2007, **363**, 294–296.